
Research report sponsored by the Re-
inforced Concrete Research Council

Horizontal Shear Connections Between Precast Beams and Cast-in-Place Slabs

By J. C. SAEMANN and GEORGE W. WASHA

This project has been concerned with the strength of the joint between precast concrete beams and cast-in-place concrete slabs. In the experimental program 42 beams and necessary control cylinders were tested in an attempt to provide information on the following variables: degree of roughness of contact surface, length of shear span, percentage of steel across the joint, effect of shear keys, position of the joint with respect to the neutral axis, and concrete compressive strength. Results obtained indicate complex relations between roughness of surface joint, percent steel across joint, and shear span.

Key words: beam; composite construction; compressive strength; connection; contact surface roughness; failure; horizontal shear connection; joint; key; precast beam; reinforced concrete; research; roughness; shear key; shear span; shear strength; slab; static test; tensile strength.

■ THE EVALUATION OF THE strength of the joint between precast concrete beams and cast-in-place concrete slabs has been the subject of considerable research. However, the ultimate strengths of bonded joints has not been well defined by the previous tests since only a few of the failures were due to horizontal shear at the joint. When the joint in a composite concrete structure is unable to transmit all internal forces from one part of the section to the other part in the same manner as if the entire section were structural concrete cast in one piece, the structure is only partially composite with stiffness characteristics between those of a fully composite and a two-piece structure.

Preliminary tests carried out by Hanson¹ on the problem of shear connections between precast beams and cast-in-place slabs indicated that the ultimate horizontal shear strength of a smooth bonded joint was about 300 psi and that of a rough bonded joint was 500 psi. In addition, it was found that the shear strength of a joint could be increased approximately 175 psi for each percent of reinforcing steel crossing the joint. These values are substantially higher than the tentative recom-

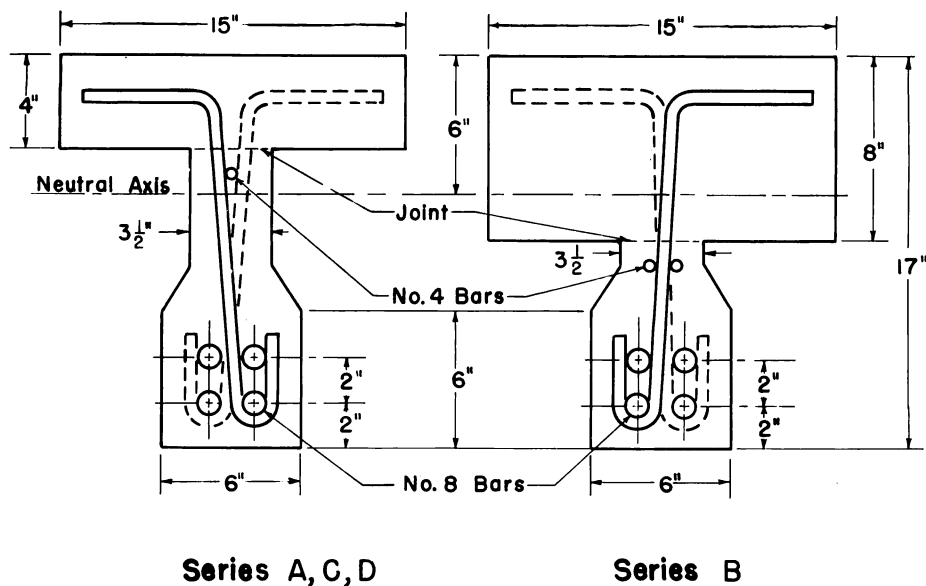


Fig. 1—Beam sections

mendations of ACI-ASCE Committee 333² which provide for the following ultimate values: 80 psi for a smooth contact surface with a minimum cross-sectional area of steel ties of 0.15 percent in each foot of span of contact area but not less than 0.20 sq in.; 320 psi for a rough contact surface with the same minimum steel requirement; an increase of 150 psi on a rough surface for each additional area of steel ties equal to 1 percent of the contact area. A comparison of the present ACI-ASCE 333 recommendations² and test results suggests the possibility of increased economy. However, before higher values are recommended, further tests and additional information are needed. The tests at the University of Wisconsin were designed to provide information on the following variables:

1. Degree of roughness of contact surface
2. Position of the joint with respect to the neutral axis
3. Length of shear span
4. Percentage of steel across the joint
5. Effect of shear keys
6. Concrete compressive strength

The total program involved the manufacture and testing of 42 T-beams and 252 6 x 12 in. compression cylinders. These static tests are to be followed by fatigue tests at Lehigh University. Final consideration of all test results may lead to a revision of the recommended stresses.

Long-time ACI member **George W. Washa** is chairman, Department of Engineering Mechanics, University of Wisconsin, Madison, Wis. In 1940 he was awarded the Wason Medal for his paper "Comparison of the Physical and Mechanical Properties of Hand Rodded and Vibrated Concrete—Made with Different Cements." Active in ACI affairs Dr. Washa is also the author of numerous papers on concrete research. Currently he is chairman of ACI Committee 516, High Pressure Steam Curing, and a member of ACI Committee 115, Research; 211, Proportioning Concrete Mixes; 213, Lightweight Aggregates and Lightweight Concrete; and ACI-ASCE Committee 333, Design and Construction of Composite Structures.

J. C. Saemann is professor, Department of Engineering Mechanics, University of Wisconsin, Madison, Wis. He has been a member of the Engineering Mechanics Department of the University of Wisconsin since 1946. Dr. Saemann is an active member of ASCE and the Highway Research Board.

VARIABLES

The variables included in this program are shown in Table 1. Not all combinations of variables were investigated. Forty-two beams were cast with 36 combinations of variables. Six check beams were included.

Fig. 1 shows the beam cross sections used with nominal dimensions indicated. The reduced breadth of web produced high horizontal shear stress in the bonded joint between the web and slab at loads well below flexural failure. The beams were designed to have the joint either 2 in. below or 2 in. above the neutral axis.

Fig. 2 shows the arrangement of stirrups (#4 bars) in beams having the maximum percentage of stirrup steel across the joint. As the nominal steel percentage decreased from 1.07 to 0.54 and from 0.54 to 0.23, the reduction in the percentage of stirrup steel across the joint in each

TABLE 1—SUMMARY OF VARIABLES

Series	Date made	No. of beams	Roughness†	Position of joint	Shear stress at flexural design load, psi§	Approximate percent steel across joint	Nominal concrete compressive strength, psi
A	Summer 1960	12	S, I, R	2 in. above neutral axis	150, 300, 450	1.07	3000
B	Summer 1960	3	I	2 in. below neutral axis	150, 300, 450	1.07	3000
C*	Summer 1961	18	S, I	2 in. above neutral axis	150, 300, 450	0, 0.07, 0.13, 0.23, 0.54	3000
D†	Summer 1962	9	S, I	2 in. above neutral axis**	150, 300, 450	0.13, 0.23	3000, 4500, 5500

*Includes two beams with keys.

†Includes one beam with keys.

‡S-smooth; I-Intermediate; R-rough

§The 150 psi shear stress was obtained with a 20 ft span, 300 psi with an 11-ft span, and 450 psi with an 8-ft span.

**Distance between neutral axis and joint decreased as concrete compressive strength increased.

TABLE 2—STIRRUP DATA

Nominal percentage of stirrup steel across the joint	Bar size	Bar spacing, in.
1.07	# 4	5
0.54	# 4	10
0.23	# 4	20
0.13	# 3	20
0.07	# 3	40
0	—	—

case was accomplished by cutting off half of the stirrups crossing the joint at a level 1 in. below the joint. The number of stirrups crossing the joint for a nominal steel percentage of 0.13 was the same as for 0.23 but #3 bars were used instead of #4 bars. As the nominal steel percentage decreased from 0.13 to 0.07 half of the #3 bars were cut off 1 in. below the joint. In summary, the information on the steel bars crossing the joint is given in Table 2. Percentage of steel was calculated by dividing the area of all stirrups crossing the joint by the total joint area.

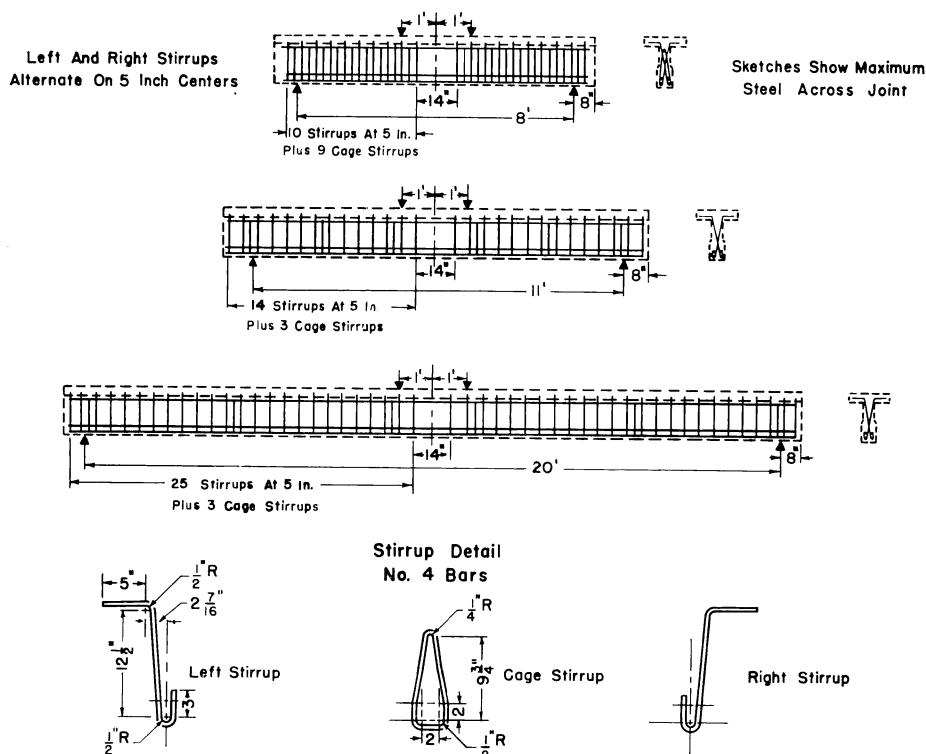


Fig. 2—Stirrup reinforcement

TABLE 3—PROPERTIES OF REINFORCING STEEL*

Size	Yield point psi	Ultimate tensile strength, psi	Elongation in 8 in., percent
#3	53,700	81,200	20
#4	42,600	58,600	29
#8	36,600	58,200	31

*Each value is the average of three test results.

MANUFACTURE OF SPECIMENS

Materials

The sand and gravel were obtained locally in Madison, Wisconsin. Both were air dried before using. The gravel was rounded and had a $\frac{3}{4}$ in. maximum size.

One brand of Type I portland cement, locally obtained, was used throughout the program. Each spring cement was purchased for the summer's work.

Properties of the reinforcing steel are given in Table 3. The #4 and #8 deformed bars were of structural grade and the #3 deformed bars of hard grade. All steel was from one shipment.

Steel fabrication

The #4, and in some cases #3, stirrup bars and #8 longitudinal bars were used in the reinforcement units shown in Fig. 3. Cage stirrups were added to reduce shear stresses below the joint. One or two #4 longitudinal bars were centered $1\frac{1}{4}$ in. below the joint to tie together the cage stirrups, stirrups crossing joint, and cut-off stirrups. All steel members of the reinforcement unit were welded together.

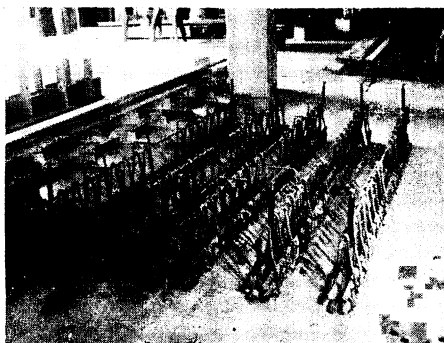


Fig. 3—Steel reinforcement

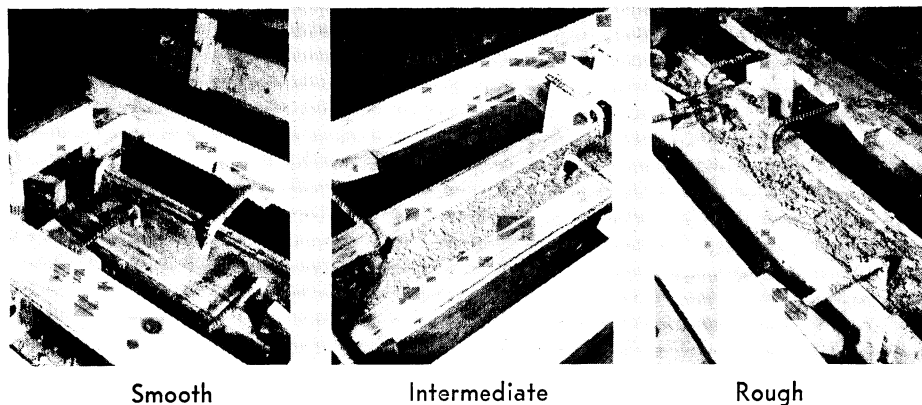


Fig. 4—Surface textures

Mixing

All concrete batches were mixed in a 6 cu ft mixer for 5 min after all materials were added. Slumps varied from $2\frac{1}{2}$ to $6\frac{1}{2}$ in. and the density between 148.2 and 151.4 lb per cu ft.

Molding procedure

Beams were cast in oiled plywood forms. The web forms were made to be filled in two layers to facilitate placing and consolidating the concrete. The bottom and 6 in. sides were assembled, steel reinforcement unit wired in place, and the lower portion of the web was filled. Then the upper sides were put in place and the remaining portion of the web was filled. Each layer of concrete was rodded and then vibrated with a 1 in. diameter internal vibrator.

A smooth finish, similar to a floated finish, was obtained by screeding. A retarding agent was used to enable brushing out the mortar between the pieces of coarse aggregate to obtain the intermediate finish. The rough finish was produced by removing particles of coarse aggregate with boards having nails protruding 1 in. Surface depressions were $\frac{1}{8}$ and $\frac{3}{8}$ in. deep, respectively, in the intermediate and rough finishes. Resulting surface finishes of the web are shown in Fig. 4.

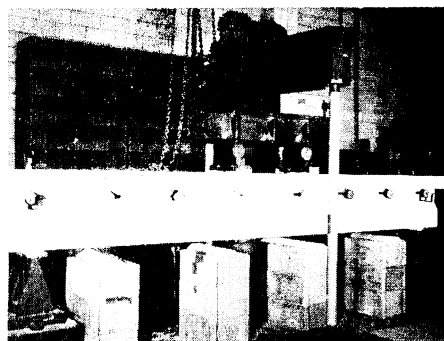
When keys were used the upper portion of the web was filled to within $1\frac{1}{4}$ in. of the top and the concrete was rodded and vibrated. Wood blocks were then nailed to the upper sides to form keys 1 in. deep, $2\frac{1}{2}$ in. long, across the full width of the joint ($3\frac{1}{2}$ in.) and spaced 5 in. on center. The remainder of the web was then filled, lightly rodded and vibrated, and the concrete surface between the wood blocks was screeded.

Keys were formed in two manners. In keys-down-beams, keys in web, the top web surface had depressions which were filled with the slab. In the keys-up-beams, keys in slab, the web surface had protrusions into the slab.

Seven days after the webs were made the slabs were cast. The concrete was rodded and then vibrated after filling the slab form.

Three 6 x 12 in. test cylinders were cast with each web and each slab. The concrete was vibrated.

Fig. 5—Test arrangement



Curing

Webs were cured under wet burlap for 7 days. Forms were removed at 2 days. Slabs and test cylinders were cured in the same manner. Beams were supported along their length at all times and were not moved from their casting position until placed in the testing machine.

TEST PROCEDURE

All beams and cylinders were tested 28 days after the slabs were cast, 35 days after the webs were cast. Stress-strain curves, ultimate compressive strengths, and moduli of elasticity at one-third ultimate stress were determined from the concrete test cylinders. The beams were tested in a hydraulic machine having a 100,000 lb capacity. Beams were supported and loaded as shown in Fig. 2, and a beam ready for test is shown in Fig. 5.

Center deflections were measured with wire-mirror-scale deflectometers. All strains were measured with a 10 in. strain gage which was seated in holes drilled in brass plugs that were attached to the concrete surface with plaster. Deflections and strains were averaged from the two sides of the beam.

Concrete stresses were approximated from concrete stress-strain curves by strain readings taken at the top and bottom of the slab and at the calculated neutral axis. Steel stresses were approximated from strain readings taken at the level of the upper and lower tension steel positions.

Slip along the joint between the slab and web was measured by dial gages reading to 0.001 in. The gages were attached to inserts cast in the bottom of the slab and were actuated by brackets attached to inserts cast in the web $1\frac{3}{4}$ in. below the joint. The insert in the slab and accompanying insert in the web were in the same vertical transverse plane and the plunger of the gage was at the same elevation as the insert in the web. Slip gages were mounted at load points, reactions, and 1.5-ft intervals between. Slip values from the two sides of the beam were averaged for plotting slip curves. When determining the load to produce 0.005 in. slip, the average of any two adjacent gages was used.

Test loads were applied in from 13 to 28 increments to failure. Loads were held constant while deflection, strain, and slip readings were taken. After some load increments, the total applied load was removed to determine set or permanent changes in deflection, strains, and slip.

DISCUSSION OF RESULTS

General

The composite beams used to evaluate the action of horizontal shear connections in flexure were designed so that high horizontal shear values at the contact surface were reached at loads well below those required for flexural failure. The horizontal shearing stress was calculated by the equation $v = VQ/Ib$, in which Q is the first moment about the neutral axis of all compression areas from the horizontal section considered to the extreme compression edge, and V is the constant live load shear between the reactions and the applied concentrated loads. The equation cannot be considered an exact representation of actual stress conditions especially after discontinuities develop due to cracking, and after slip has started. The calculated stresses, however, do provide a common basis for comparison and are so used.

The concrete in the webs and slabs of 40 of the test specimens was designed for a compressive strength of 3000 psi. The actual average compressive strength of the concrete in the webs was 3140 psi with the actual values varying between a minimum of 2530 psi to a maximum of 3800 psi, and with 34 of the webs having ultimate compressive strengths in the range ± 15 percent from the average. The average modulus of elasticity for the concrete in the webs was 3,150,000 psi. In the 40 slabs the average ultimate compressive strength was 3160 psi with values varying between 2680 to 3870 psi and with 37 of the slabs having ultimate compressive strengths in the range ± 15 percent from the average. The average modulus of elasticity for the concrete in the slabs was 3,180,000 psi. The remaining two beams were designed for nominal ultimate compressive strengths of 4500 and 5500 psi. The actual compressive strengths and moduli of elasticity for all beams are given in Table 4 along with a summary of the important results obtained for each beam tested. The beam test results are given at design load, at a slip of 0.005 in., and at ultimate load. The slip of 0.005 in. has been considered by Hanson¹ to be a critical value at which beam deflection curves begin to deviate from a smooth curve.

Some of the measured steel stresses at design load, Table 4, varied considerably from the assigned value of 18,000 psi. Probable reasons for these variations were: calculation of stresses from strains measured on concrete surfaces; cracking of concrete in tension within or outside of the gage length; disregard for tension carried by the concrete.

The results for Beam 10C were discarded because they varied considerably from those for replicate Beams 5D and 6D. The measured load at ultimate for Beam 11C was significantly lower than that of its replicate 2D, but the average was used because all other results for the two beams were in reasonable agreement. In all other instances of replication the comparable values showed reasonable agreement. When the

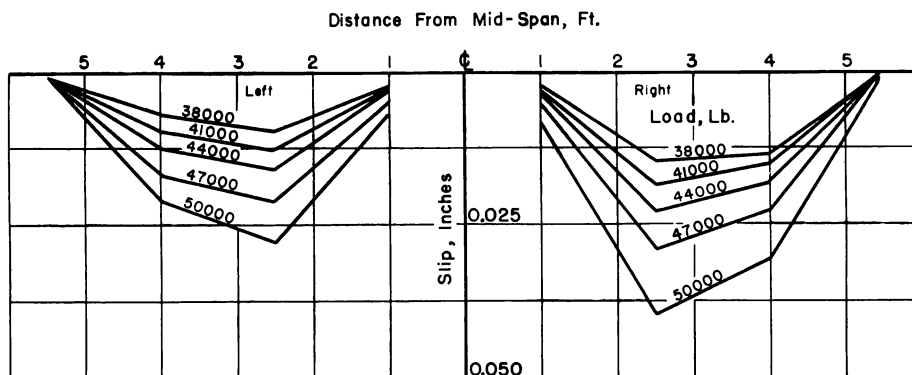


Fig. 6—Development of slip

results from Table 4 were plotted, average values were used whenever there was more than one beam per variable.

Performance characteristics of test beams

After a few increments of load, initial flexural cracking at the bottom of the beam was noted in all tests. As the loading increased more cracks were formed and those previously formed became deeper and inclined toward the center. Additional loading caused the cracks to reach the joint between the web and slab and later, in some beams, to travel along the joint. The motion between the web and slab was read from the slip gages and typical slip curves are shown in Fig. 6. The slip variation at ultimate load is not shown because it was not possible to obtain readings at that load. The curves do show that slip increased as the load increased, that maximum slips were usually located about $2\frac{1}{2}$ ft each side of the center of the beam, and that the development of slip was not symmetrical with respect to the center of the beam. The magnitude of slip at ultimate load was generally least for the 20-ft beams, in most cases less than 0.005 in.

Three fundamental types of failure were obtained: tension, shear, and tension-shear as noted in Table 4. The tensile failure was observed in the long beams (20 ft) for all roughness conditions when 1.12 percent steel across the joint was used, and for an intermediate roughness condition when 0.15 percent steel was used. At ultimate the maximum tensile steel strain exceeded the strain at yield point and the maximum slip was generally less than 0.005 in. Little horizontal cracking between web and slab was observed and no horizontal cracks at the joint were noted on the end surfaces. Loading of the beams that failed in tension was continued until crushing of the concrete took place. A typical failure is shown in Fig. 7.

Most of the short (8 ft) and intermediate length (11 ft) beams had shear failures. All exceptions, beams with more than 1.0 percent steel

TABLE 4—SUMMARY

Beam		L, ft	Rough- ness	Steel across joint, percent	Shear span Effective depth	Concrete properties				Calcu- lated flexural design load, lb
						Web		Slab		
No.	Series					f_c' , psi	E 10 ⁶ psi	f_c' , psi	E psi	
9	A	20	S	1.12	7.71	2640	2.84	3060	3.29	12,900
1	C	20	S	0.58	7.71	3160	3.10	2950	2.99	12,900
6	C	20	S	0.27	7.71	2870	2.90	3040	2.98	12,900
5	A	20	I	1.12	7.71	2850	3.39	2970	3.00	12,900
1	D	20	I	0.15	7.71	3520	3.17	3380	3.31	12,900
11	A	20	R	1.12	7.71	2990	3.12	3020	3.25	12,900
3	A	20	R	1.12	7.71	2790	2.82	2910	3.13	12,900
4	A	11	S	1.08	3.86	2810	3.23	2720	3.02	25,800
12	A	11	S	1.08	3.86	3070	3.30	2790	3.21	25,800
2	C	11	S	0.54	3.86	2970	3.00	3300	2.97	25,800
7	C	11	S	0.23	3.86	3340	3.09	2810	2.93	25,800
3	D	11	S	0.13	3.86	3720	3.44	3590	3.32	25,800
2	A	11	I	1.08	3.86	2530	2.83	2680	2.88	25,800
3	C	11	I	0.54	3.86	3080	3.11	3070	3.055	25,800
8	C	11	I	0.23	3.86	2790	2.905	2980	3.055	25,800
11	C	11	I	0.13	3.86	2950	3.035	2870	2.94	25,800
2	D	11	I	0.13	3.86	3740	3.67	3550	3.38	25,800
13	C	11	I	0.08	3.86	3730	3.275	3420	3.08	25,800
15	C	11	I	0.00	3.86	3030	2.885	3220	3.16	25,800
8	A	11	R	1.08	3.86	2920	3.14	2950	3.17	25,800
4	D	11	KD	0.13	3.86	3470	3.56	3530	3.52	25,800
1	A	8	S	1.02	2.57	2860	2.89	2710	2.82	38,600
4	C	8	S	0.51	2.57	3170	2.935	3320	3.26	38,600
9	C	8	S	0.20	2.57	3090	2.945	3180	3.315	38,600
7	D	8	S	0.11	2.57	3800	3.61	3750	3.68	38,600
7	A	8	I	1.02	2.57	2890	3.21	3050	3.28	38,600
10	A	8	I	1.02	2.57	3060	3.19	2870	3.09	38,600
5	C	8	I	0.51	2.57	3020	2.96	3260	3.20	38,600
10	C	8	I	0.20	2.57	3490	2.77	3120	3.155	38,600
5	D	8	I	0.20	2.57	3390	3.48	3580	3.51	38,600
6	D	8	I	0.20	2.57	3680	3.61	3870	3.69	38,600
12	C	8	I	0.11	2.57	2980	3.10	3470	3.125	38,600
8	D	8	I	0.11	2.57	4610	3.65	4720	3.92	39,000
9	D	8	I	0.11	2.57	5420	4.13	4900	3.71	39,400
14	C	8	I	0.06	2.57	3130	3.17	2870	3.14	38,600
16	C	8	I	0.00	2.57	3030	2.97	3060	3.00	38,600
6	A	8	R	1.02	2.57	2900	3.02	3610	3.44	38,600
17	C	8	KD	0.11	2.57	3190	3.13	3290	3.04	38,600
18	C	8	KU	0.11	2.57	3290	3.13	3210	3.06	38,600
13	B	20	I	1.12	7.71	3450	3.39	3100	3.23	13,100
14	B	11	I	1.08	3.86	3060	3.29	3050	3.18	26,200
15	B	8	I	1.02	2.57	3280	3.42	3230	3.26	39,300

*These stresses were calculated using measured superimposed live loads only.

OF RESULTS

At design load			At 0.005 in. slip		Calculated flexural live load at ultimate, lb	At ultimate		Type of failure
Measured f_c top of slab, psi	Measured f_s lower steel, psi	Nominal calculated V, psi	Live load, lb	Calculated V^* , psi		Measured live load, lb	Calculated V^* , psi	
1400 1170	16,000 18,400	150 150	— 21,550	— 251	25,600 25,400	25,900 25,600	302 298	Tension Shear
1235 1390 1425	15,000 21,400 21,100	150 150 150	23,000 — —	268 — —	25,500 25,400 25,900	23,000 24,500 26,900	268 286 314	Shear Tension Tension
1300 1330	14,000 17,800	150 150	24,350 24,750	284 289	25,500 25,400	25,700 25,700	300 300	Tension Tension
1260 1320	14,700 16,100	300 300	24,600 30,500	287 356	52,400 52,600	53,000 50,900	618 594	Tension-shear Tension-shear
1250 1210 1230	17,200 15,600 19,000	300 300 300	26,300 24,000 24,200	307 280 282	53,800 52,600 54,400	41,100 38,000 35,300	479 443 412	Shear Shear Shear
1200 1260	16,000 15,800	300 300	32,000 30,800	373 359	52,300 53,300	53,000 51,000	618 595	Tension-shear Shear
1230 1260 1250	15,300 14,300 17,800	300 300 300	31,000 25,450 28,200	362 297 328	53,100 52,800 54,300	47,000 34,000 47,000	548 396 548	Shear Shear Shear
1240 1250	19,100 16,250	300 300	22,350 28,200	261 329	54,100 53,700	36,000 36,000	420 420	Shear Shear
1310 1480	15,700 12,700	300 300	37,000 23,400	431 273	53,000 54,300	53,000 44,000	618 513	Tension-shear Shear
1160 1240 1270	16,000 14,800 12,600	450 450 450	34,850 26,650 28,950	407 311 338	79,200 81,500 81,100	76,400 60,000 48,000	891 699 560	Shear Shear Shear
1125 1290	22,400 20,700	450 450	32,200 41,800	375 488	82,700 80,600	51,200 75,100	597 876	Shear Tension-shear
1270 1320 1270	24,600 21,000 13,000	450 450 450	46,200 31,500 26,500	538 367 309	79,900 81,300 80,900	80,040 80,000 57,800	934 934 674	Tension-shear Shear Shear
1420 1490	17,300 20,250	450 450	37,300 44,000	435 513	82,200 82,900	76,400 76,000	891 885	Shear Shear
1270 1520 1275	20,000 12,000 17,200	450 450 450	39,450 42,000 51,000	460 487 598	81,900 84,500 84,800	69,000 76,000 78,000	805 881 915	Shear Shear Shear
1220 1310	19,600 18,300	450 450	40,000 38,000	466 443	79,900 80,600	62,000 52,000	723 606	Shear Shear
1280 1350 1150	20,200 17,900 18,300	450 450 450	51,000 35,100 38,600	595 410 450	82,300 81,400 81,200	81,700 64,000 75,300	953 746 878	Tension-shear Shear Shear
1350 1360	13,500 13,300	150 300	26,000 35,000	324 437	26,700 56,100	27,800 59,700	347 745	Tensile Tension-shear
1360	17,100	450	41,500	518	85,800	90,500	1128	Tension-shear

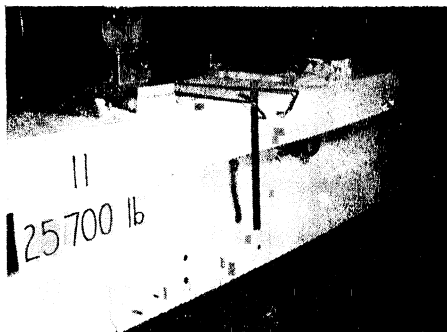


Fig. 7—Tension failure of Beam 11A

across the joint and with all degrees of roughness, failed because of a combination of high shear and tensile stresses. When beams failed primarily in shear the flexural cracks inclined toward the center of the beam and when they came in contact with the slab they followed the joint. As loading continued the length of the horizontal crack increased until it progressed nearly the entire length of the beam. The crack across one end of the beam was evident at ultimate load in all shear failures, and in some beams they were evident on both ends. At ultimate the horizontal displacement of the top slab with respect to the web usually varied between $\frac{1}{8}$ and $\frac{1}{2}$ in. Examination of failures indicated that in most cases some concrete from the web adhered to the flange. No loose aggregate particles were noted. Typical failures are shown in Fig. 8a and 8b. Final failure was usually accompanied by a compression failure in the web as shown at the left in Fig. 8b.

As the shear caused slip to develop between flange and web the beam began to act as a partially composite member. This action is shown in Fig. 9 where the strain distribution is plotted for a series of increasing loads. It may be noted that for the first three loads the strain distribution was linear with the neutral axis approximately 6 in. below the top of the beam or 2 in. below the joint. At the next load, 31,500 lb, a



Fig. 8a—Shear failure of Beam 13C

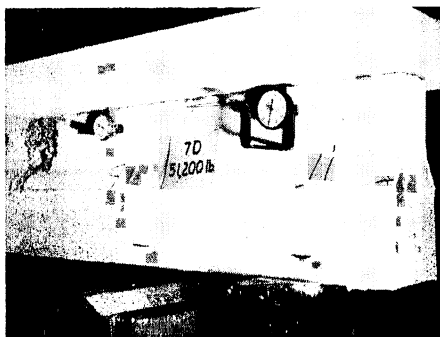


Fig. 8b—Shear failure of Beam 7D

discontinuity in the strain distribution at the joint is apparent. At the higher loads this discontinuity is pronounced and it is apparent that two-beam action exists. The center of rotation of the flexural strains in the slab, for the three largest loads, appears to be located slightly below midheight of the slab, and the center of rotation of the flexural strains in the web appears to be about 1 in. above the center line of the upper tension steel. During the test two-beam action was confirmed by the appearance of tensile cracks on the bottom surface of the slab.

The failure of a beam with the keys in the web is shown in Fig. 10. The shear failure took place along the bottom of keys. The web compression failure and the tensile crack in the slab are shown.

The third type of failure, tension-shear, was obtained for all 8 and 11-ft beams containing over 1 percent steel across the joint and for all three conditions of surface roughness except for the 8-ft beam with a smooth joint which failed in shear. At ultimate, the beams showing a tension-shear type failure had tensile steel stresses beyond the yield

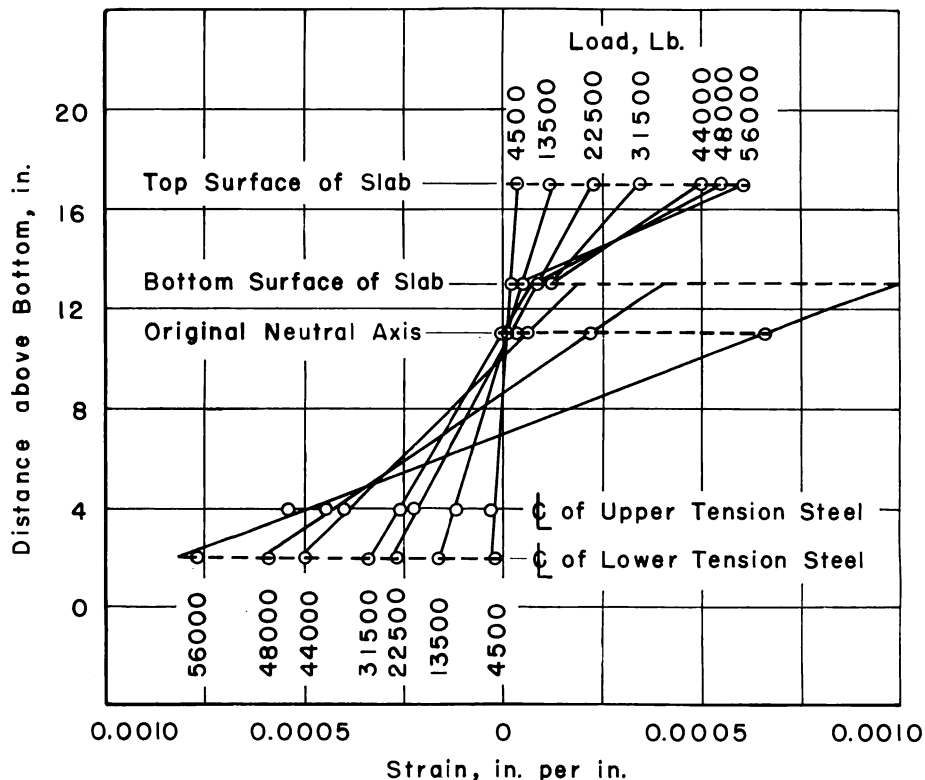


Fig. 9—Strain distribution showing two-beam action

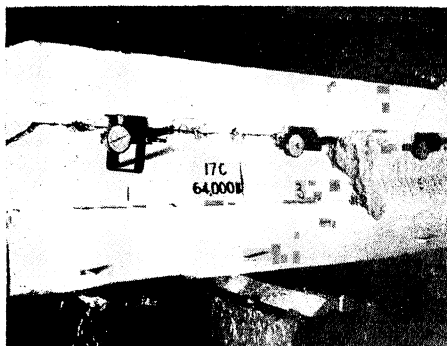


Fig. 10—Shear failure of Beam 17C

point and slip values greatly in excess of 0.005 in. Loading was continued until compressive crushing of the concrete occurred.

Relation between shear stress and position of neutral axis

The effect of the position of the joint in relation to the neutral axis was investigated briefly by making three beams in Series B, one for each span, with the joint 2 in. below the neutral axis and comparing results with beams similar in all respects except that the joint was 2 in. above the neutral axis. The analysis may be readily made by comparing results for Beams 13B with 5A, 14B with 2A, and 15B with the average of 7A and 10A in Table 4. The beams with the joint 2 in. below the neutral axis averaged about 14 percent stronger than the beams with the joint above the neutral axis. However, if a correction is made to take into account the greater concrete strength of Beams 13B, 14B, and 15B, the increase is about 10 percent. It should be noted that this increase was obtained only with a much heavier beam in Series B, with a slab 8 in. thick as against the 4 in. thickness used in the comparison beams. Also, in addition to the four #8 tensile bars, the Series B beams had two #4 bars below the neutral axis while the Series A beams had one #4 bar above the neutral axis.

Relation between shear stress and center deflection

The curves in Fig. 11 show the effects of many important variables. Each curve is identified by its beam number (Table 4) or two numbers if an average curve is shown. Beams failing in tension or tension-shear have arrows at the ends of curves signifying increasing deflection at essentially constant load. In general, it may be noted that the 8 and 11 ft intermediate beams showed greater deflections and a greater tendency for two-beam action as the percentage steel across the joint increased. The combination of higher loads and greater deflections produced greater toughness and a more desirable failure. Except for the beams with the highest percent steel across the joint the start of two-

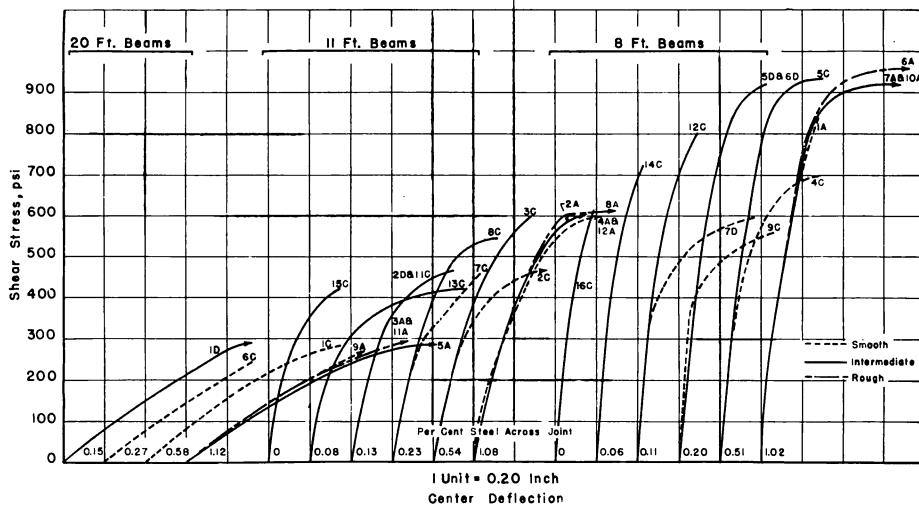


Fig. 11—Shear stress versus deflection

beam action for beams with a smooth joint took place at much lower loads than for the beams with a joint of intermediate roughness.

The curves for the 20-ft beams are nearly alike and all show a maximum shear stress at slightly less than 300 psi, regardless of the percentage steel across the joint or the degree of surface roughness. The curves for the 11-ft beams show, in general, that for an intermediate surface roughness the maximum shear stress increased from about 400 to 600 psi as the percent steel across the joint increased from zero to 1.08 percent. Also, it is evident that smooth surfaces resulted in lower ultimate shear stress values and that results for rough surfaces were nearly the same as those for intermediate surfaces. In general, similar statements may be made for the 8-ft beams. The ultimate shear stresses increased from 600 to slightly over 900 psi as the percent steel across the joint increased from zero to 1.02 percent for the beams with the intermediate roughness.

The curves in Fig. 12 show the effect of surface roughness on the ultimate shear stress. The ultimate shear stress increased slightly as the roughness increased from smooth to intermediate. In comparing Specimen 4D with the average curve for Specimens 2D and 11C it should be noted that Specimen 2D failed at a higher shear stress and Specimen 11C failed at a lower shear stress than the shear stress at failure for Specimen 4D. The 8-ft beams showed a marked increase in ultimate shear stress as the roughness increased from smooth to intermediate. The beam with the intermediate roughness had a better ultimate shear stress than the keyed beam with the keys in the web but a lower shear stress than the keyed beam with the keys in the slab.

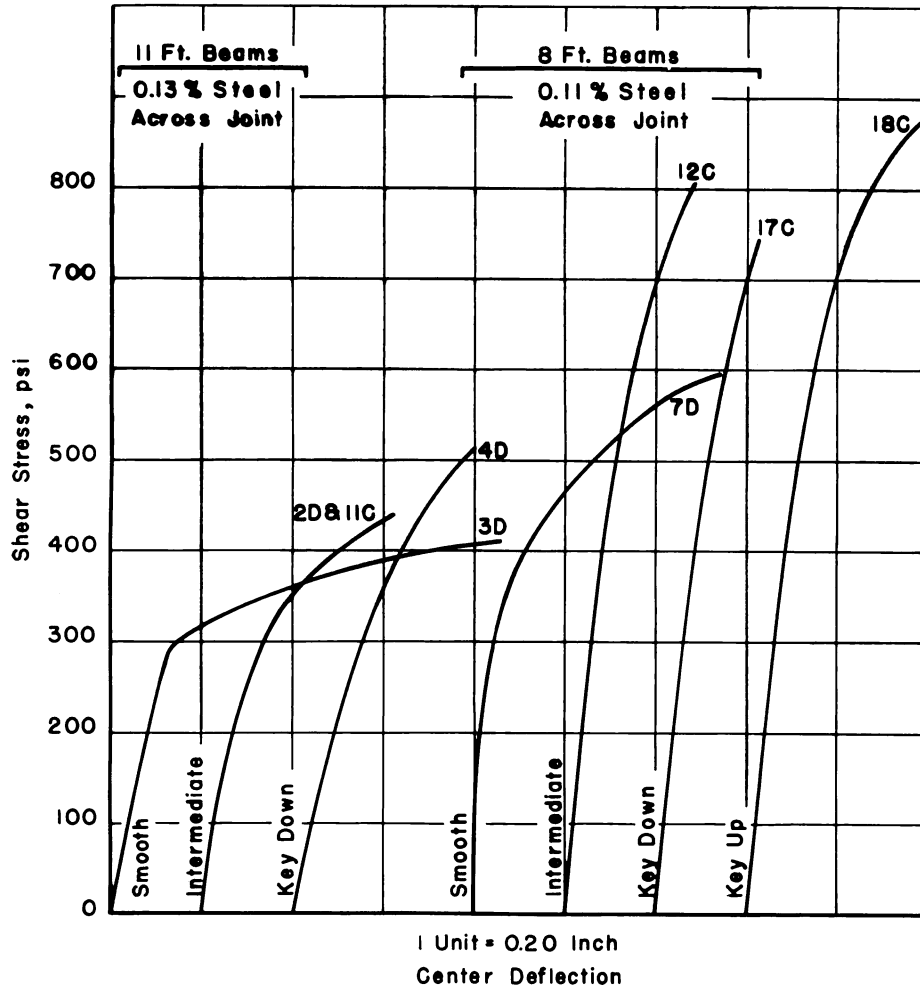


Fig. 12—Effect of roughness on shear stress versus deflection

Relation between shear stress and maximum slip

The curves relating maximum slip (average of two adjacent readings at a given load) to shear stress are shown in Fig. 13-15. These curves show that for the 20-ft beams the ultimate shear stresses were very close to 300 psi for all conditions and that the maximum slip values were usually small. The 8 and 11-ft beams generally showed an increase in ultimate shear stress as the percent of steel across the joint increased and as the degree of roughness increased. The maximum slip at ultimate exceeded 0.02 in. for all 8 and 11 ft smooth and intermediate beams. The 8 and 11 ft rough beams, with slightly more than 1.0 percent steel across the joint, had maximum slips at ultimate of 0.02 in. or less. The curves in Fig. 15 show that the beams with a joint of intermediate roughness were similar to keyed beams, and that the beams with a smooth joint were definitely inferior.

Relation between concrete compressive strength and shear stress

The results of a limited program concerned with the effect of compressive strength are presented in Fig. 16-18. While the curves in Fig. 16 and 17 show similar characteristics in each case they also show that the ultimate shear stress increased slightly as the concrete compressive strength increased. This may also be seen in Fig. 18 where the shear

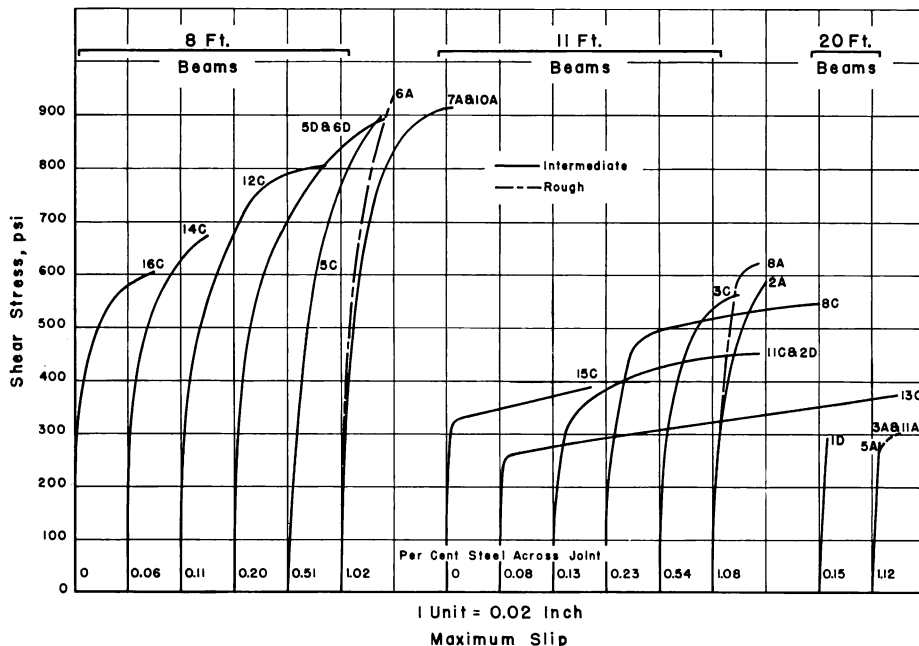


Fig. 13—Shear stress versus slip for intermediate and rough beams

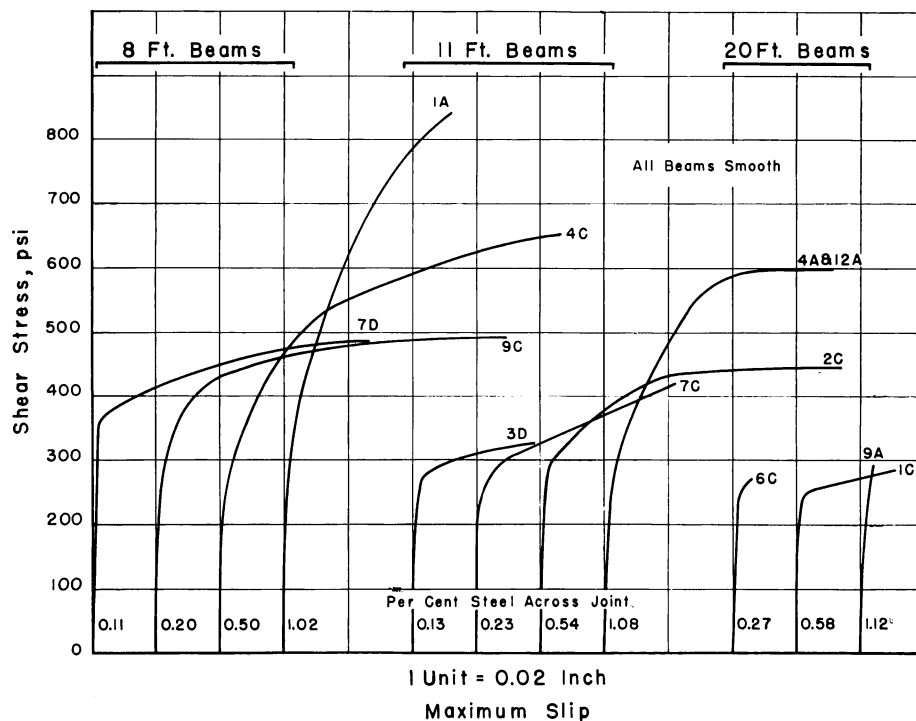


Fig. 14—Shear stress versus slip for smooth beams

stress is plotted against the minimum concrete compressive strength (lower of the two values for the web and slab concrete) at 0.005 in. slip and also at ultimate load.

Relation between shear stress and percent steel across the joint

The effect of increasing the amount of steel across the joint on the shear stress at 0.005 in. slip is shown in Fig. 19, and the shear stress at ultimate is shown in Fig. 20. It may be noted that for a given roughness and for a given length the shear stress at 0.005 in. slip increased as the percent steel across the joint increased, except for the 20-ft beams where no appreciable effect on the shear stress at 0.005 in. slip or at ultimate load was shown. The shear stress at ultimate for the smooth 8 and 11-ft beams increased as a straight line function of the percent steel across the joint. The curves for the intermediate 8 and 11-ft beams in Fig. 20 show that small amounts of steel across the joint, from zero to 0.20 percent, were effective in increasing the shear stress at ultimate load. Increasing the amount of steel beyond 0.20 percent produced only slight increases in the shear stress at ultimate load.

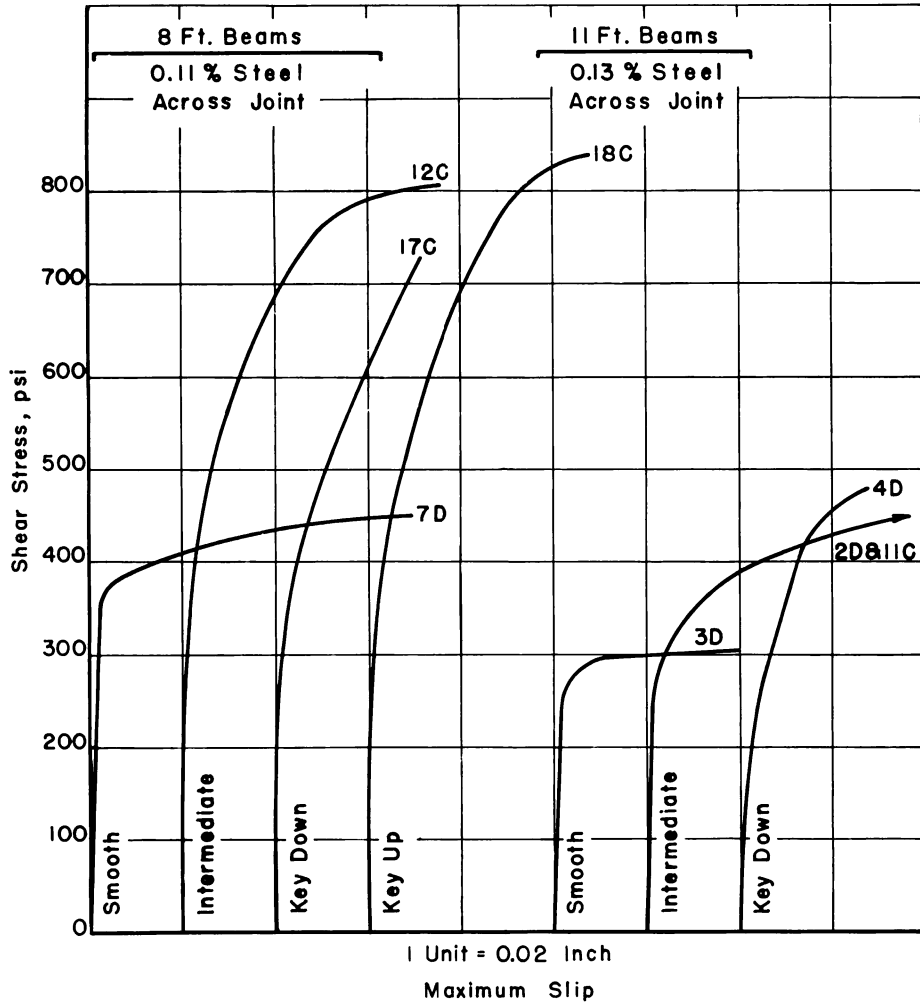


Fig. 15—Effect of roughness on shear stress versus slip

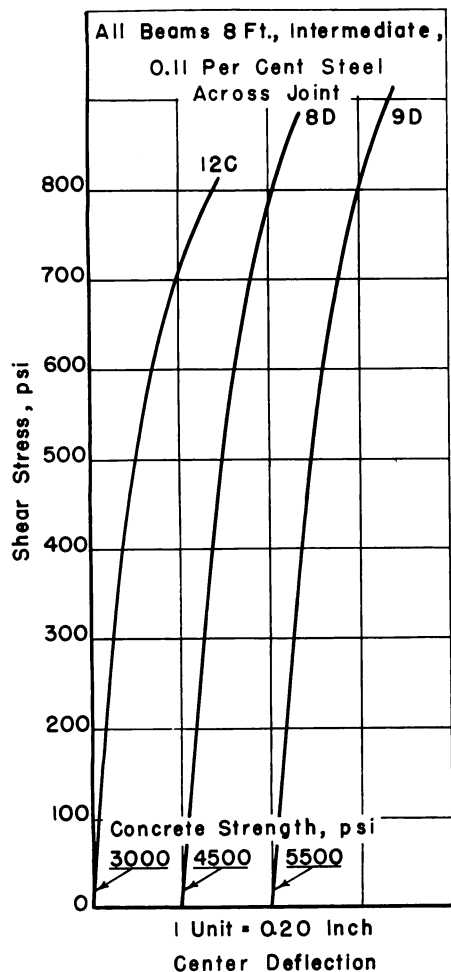


Fig. 16—Effect of concrete strength on shear stress versus deflection

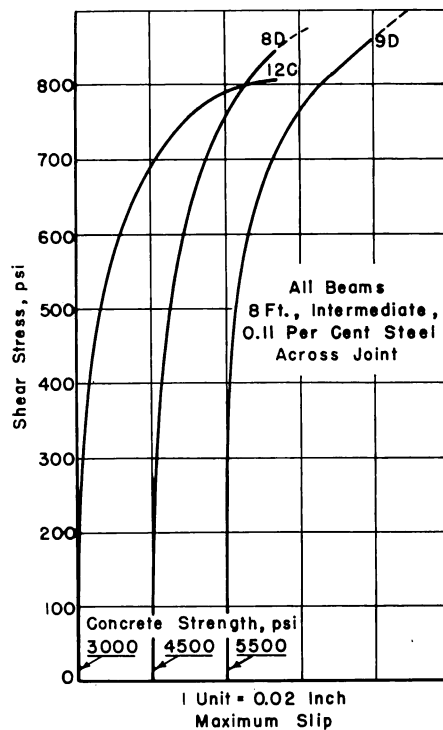


Fig. 17—Effect of concrete strength on shear stress versus slip

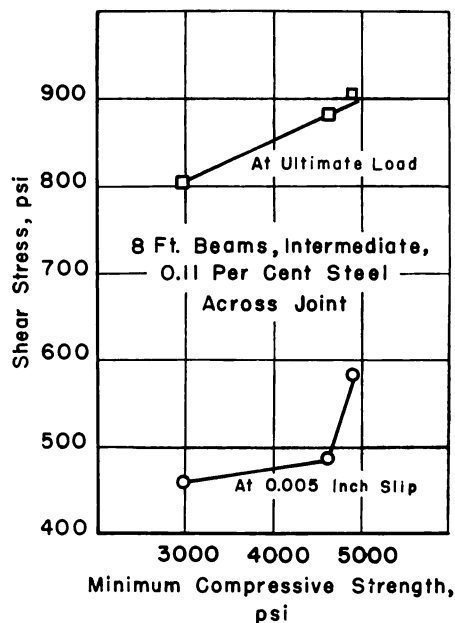


Fig. 18 (right) — Shear stress versus minimum concrete strength

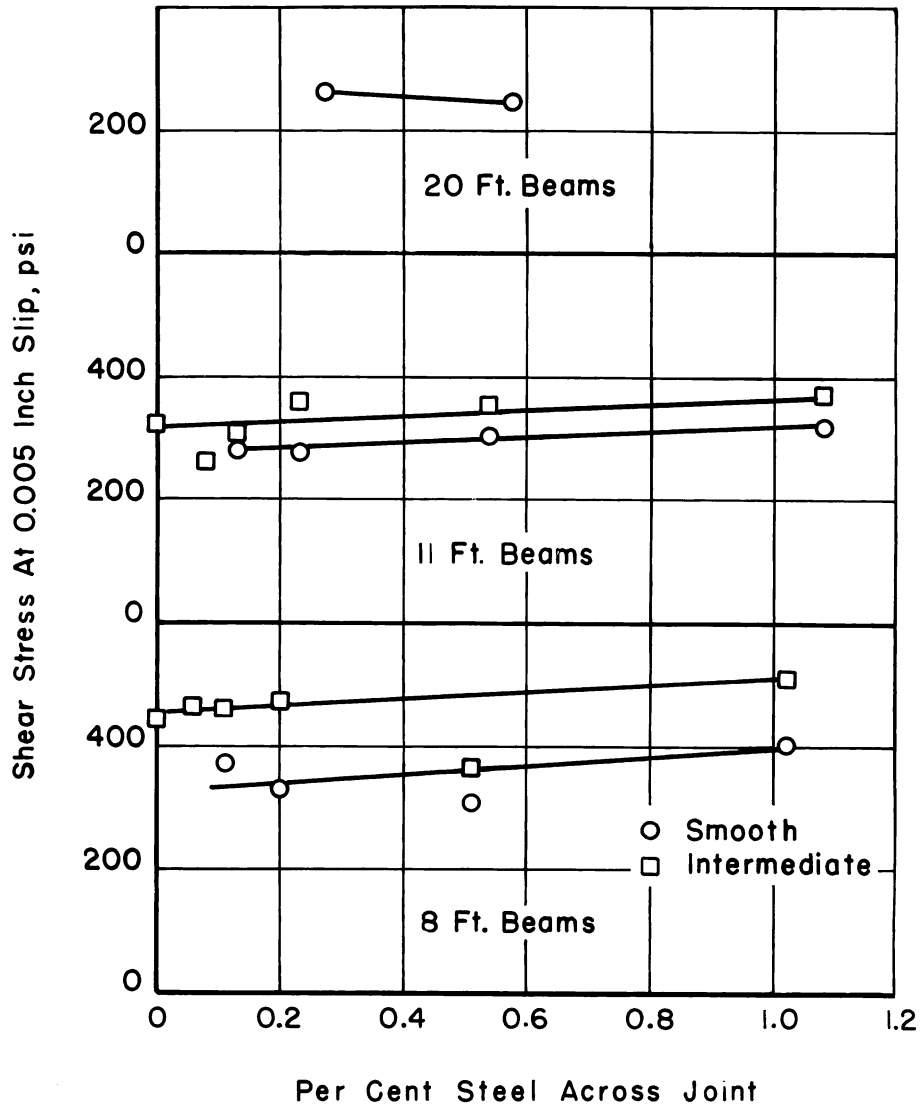


Fig. 19—Shear stress at 0.005 in. slip versus steel across joint

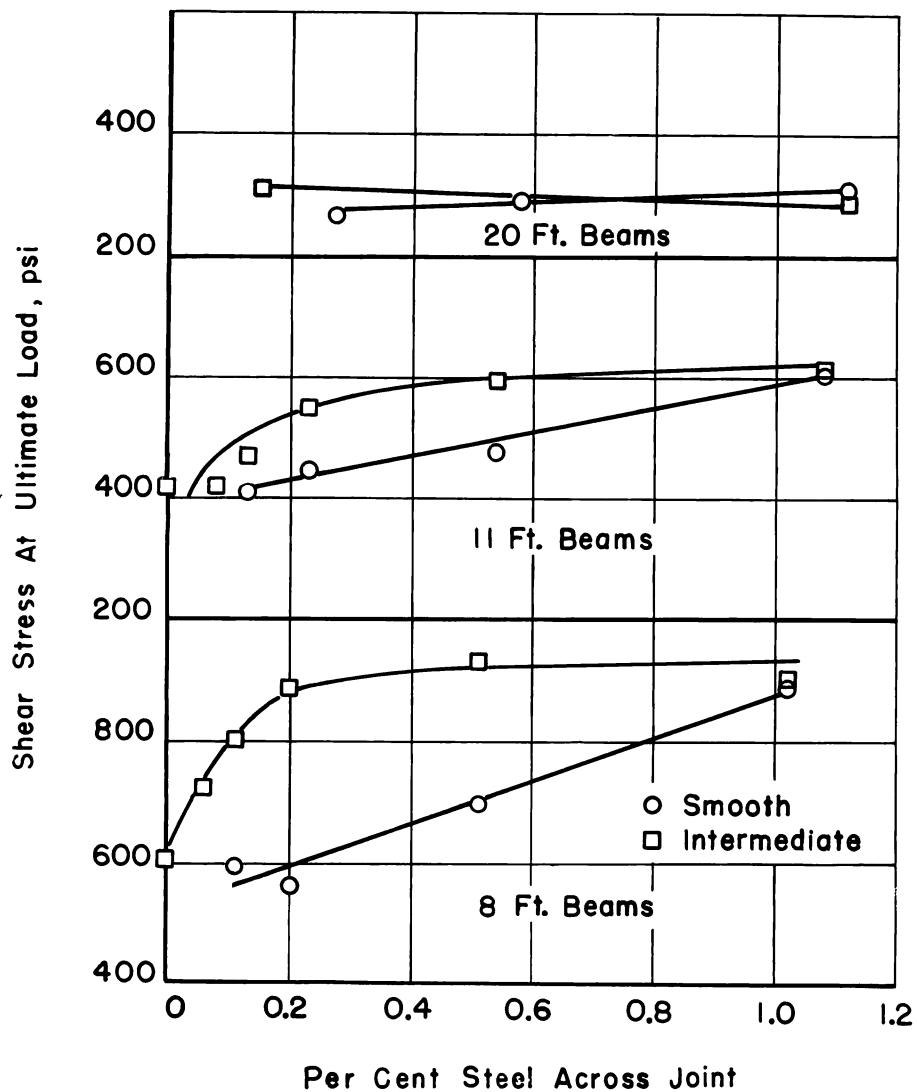


Fig. 20—Shear stress at ultimate load versus steel across joint

Relation between percent steel across joint and the ratio of ultimate load to $1.8 \times$ design load (straight line theory of flexure) based on moment

The test results plotted in Fig. 21 show that when at least 0.15 percent steel was placed across the joint the actual ultimate strength exceeded the value $1.8 \times$ design load except for five beams which all had a smooth joint. When the amount of steel exceeded 0.60 percent, the ultimate load exceeded the value $1.8 \times$ design load in every case. The Series B beams showed the best results with ratios between 1.18 and 1.28. In summary, it may be noted that the ratio exceeded 1.0 for all beams with an intermediate or rough contact surface when the amount of steel across the joint exceeded 0.15 percent..

Relation between the ultimate shear strength and the ratio of shear span to effective depth

Fig. 22 shows that the ultimate shear strength Y decreases as: the ratio of shear span* to effective depth X increases, the percent steel across the Joint P decreases, and the surface roughness at the joint decreases. The equation of the curve for zero percent steel is:

$$Y = \frac{2700}{X + 5}$$

which is the same equation recommended by Mattock and Kaar³ for a rough bonded contact surface with no steel across the joint. The effect of the steel is considered in the second part of the equation:

$$300P \left(\frac{33 - X}{X^2 + 6X + 5} \right)$$

Roughness of joint is not considered since its effect is variable and becomes less as more steel is placed across the joint and as X increases.

Fig. 22 shows that all test results exceed the computed values. It should be noted that steel additions are beneficial at low values of X

*Shear span is the distance from a reaction to the first applied concentrated load.

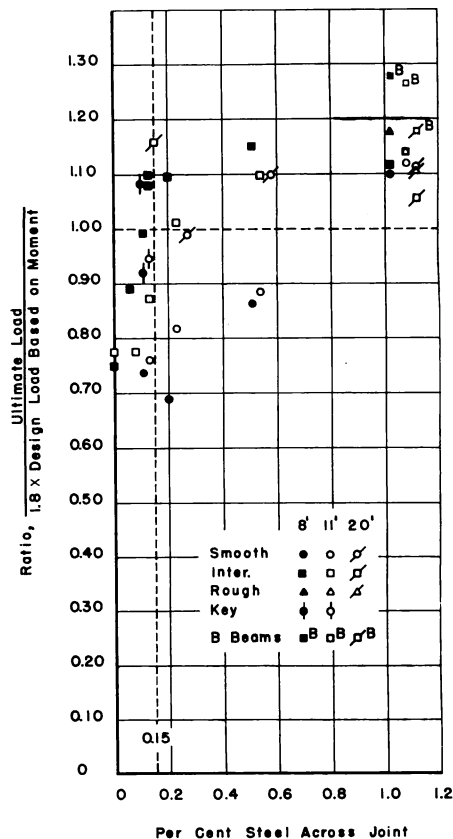


Fig. 21—Effect of steel across joint on ultimate load/ $1.8 \times$ design load based on moment

and are of small value for the larger values of X . This fact is not in agreement with the recommendations of Section 205.3 of ACI-ASCE Committee 333.² This recommendation permits the ultimate shear strength on a rough joint to be increased at a rate of 150 psi for each additional area of steel ties equal to 1 percent of the contact area, but it does not take the ratio of shear span to effective depth into consideration. The test results also do not substantiate the recommended large

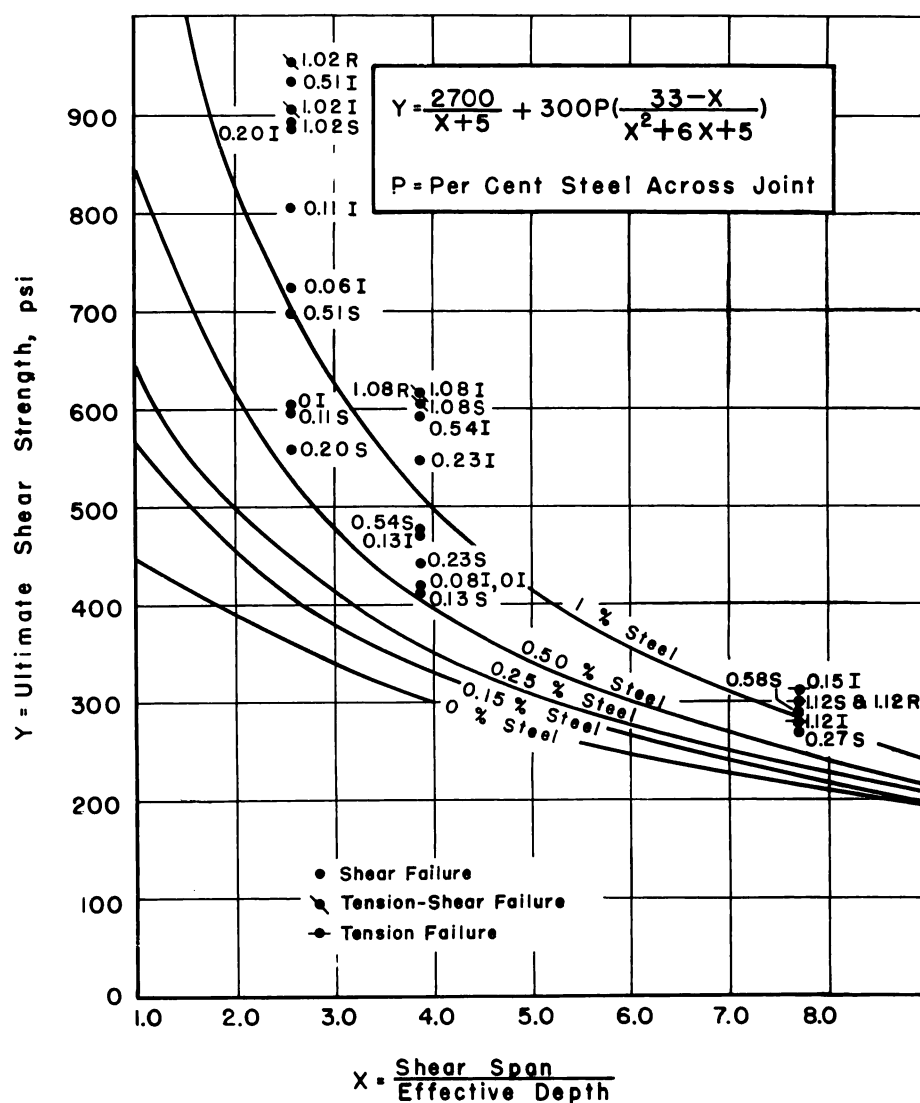


Fig. 22—Effect of shear span/effective depth and steel across joint on ultimate shear strength

difference in the ultimate shear stress at the joint, varying from 80 psi for a smooth surface to 320 psi for a rough surface when the minimum steel requirements are satisfied.

Consequently, it appears that the ratio of shear span to effective depth should be considered when allowable or ultimate shear strength values are recommended regardless of the amount of steel across the joint.

CONCLUSIONS

1. In general, the ultimate shear strength of the joint:
 - (a) Increased for the 8 and 11-ft beams as the contact surface roughness increased from smooth to intermediate.
 - (b) Increased considerably for the 8 and 11-ft beams with a smooth contact surface as the amount of stirrup steel across the joint increased.
 - (c) Increased considerably for the 8 and 11-ft beams with an intermediate contact surface as the amount of stirrup steel across the joint increased up to about 0.20 percent.
 - (d) Showed little change for all 20-ft beams as contact surface roughness and the amount of stirrup steel across the joint increased.
 - (e) Increased as the ratio of shear span to effective depth decreased.
2. Beams with an intermediate rough surface had ultimate shear strengths approximately equal to those for beams with keys. Keys in the flange were slightly more effective than keys in the web.
3. An increase in the concrete strength from 3000 to 5500 psi increased only slightly the ultimate shear strength of the joint.
4. All beams containing more than 0.15 percent steel and having an intermediate or rough contact surface carried an ultimate load greater than $1.8 \times$ design load based on moment.
5. The beams with the joint 2 in. below the neutral axis were somewhat stronger than comparable beams with the joint 2 in. above the neutral axis.
6. Three types of failure were obtained in these tests. The longest beams (20 ft) required a calculated horizontal shear stress of approximately 300 psi to develop ultimate flexural strength. Tension failures (yielding) were noted for these beams when a smooth surface was combined with a high percentage of steel crossing the joint, or when sufficient roughness was present. The 11-ft beams required a calculated horizontal shear stress of approximately 600 psi to develop the ultimate flexural strength. These beams failed with a combination tension-shear failure when about 1 percent steel was used across the joint regardless of the surface roughness. The 8-ft beams which similarly required about

900 psi for flexural ultimate failed in a combination of tension-shear only when roughness and high amounts of steel were combined. All other beams failed primarily because of the shear stress on the joint.

7. The curves relating ultimate shear strength to the percent steel across the joint and to the ratio of shear span to effective depth show the need for considering this ratio in addition to variables previously considered.

8. On the basis of the test results ultimate shear strength (Y) may be given by:

$$Y = \frac{2700}{X + 5} + 300P \left(\frac{33 - X}{X^2 + 6X + 5} \right)$$

This equation takes into account the percent steel across the Joint P and the ratio of shear span to effective depth X . Roughness of joint is not considered since its effect is variable and becomes less as more steel is placed across the joint and as X increases. However, the ultimate shear strength does increase as the roughness of the joint is increased.

ACKNOWLEDGMENTS

This research program was financed by funds from the State Highway Commission of Wisconsin in cooperation with the U.S. Department of Commerce-Bureau of Public Roads, the Reinforced Concrete Research Council, and the University of Wisconsin Engineering Experiment Station. The interest and council of T. Germundsson, N. W. Hanson, H. B. Schultz, A. Tedesko, and I. M. Viest has been very helpful. The effective cooperation of all student and staff members throughout the program is gratefully acknowledged.

REFERENCES

1. Hanson, N. W., "Precast-Prestressed Concrete Bridges. 2—Horizontal Shear Connections," *Journal, PCA Research and Development Laboratories*, V. 2, No. 2, May 1960, pp. 38-58. *PCA Development Bulletin D35*.
2. ACI-ASCE Committee 333, "Tentative Recommendations for Design of Composite Beams and Girders, for Buildings" *ACI JOURNAL, Proceedings* V. 57, No. 6, Dec. 1960, pp. 609-628; see also *Proceedings, ASCE*, V. 86, ST12, Dec. 1960, pp. 73-92.
3. Mattack, A. H., and Kaar, P. H., "Precast-Prestressed Concrete Bridges. 4—Shear Tests of Continuous Girders," *Journal, PCA Research and Development Laboratories*, V. 3, No. 1, Jan. 1961, pp. 47-56. *PCA Development Bulletin D45*.
4. Grossfield, B., and Birnstiel, C., "Tests of T-Beams with Precast Webs and Cast-in-Place Flanges," *ACI JOURNAL, Proceedings* V. 59, No. 6, June 1962, pp. 843-851.

Received by the Institute July 18, 1963. Title No. 61-69 is a part of copyrighted Journal of the American Concrete Institute, *Proceedings* V. 61, No. 11, Nov. 1964. Separate prints are available at 75 cents each, cash with order.

Discussion of this paper should reach ACI headquarters in triplicate by Feb. 1, 1965, for publication in the Part 2 June 1965 JOURNAL.

Sinopsis — Résumés — Zusammenfassung

Conexiones por Cortante Horizontal entre Vigas Precoladas y Losas Coladas en el Lugar

Este proyecto trata sobre la resistencia de la junta entre vigas precoladas y losas coladas en el lugar. En el programa experimental se ensayaron 42 vigas y los cilindros de control necesarios en un intento de suministrar información en las siguientes variables: grado de rugosidad de la superficie de contacto, longitud del claro de cortante, cuantía del acero a través de la unión, efecto de los conectores por cortante, posición de la unión con respecto al eje neutro, y resistencia a compresión del concreto. Los resultados obtenidos indican relaciones complejas entre la rugosidad de la superficie de la junta, porcentaje del acero a través de la junta, y claro de cortante.

Cisaillement Horizontal aux Joints par Contact entre les Poutres de Béton Prémoulées et des Dalles Coulées en Place

On tente de déterminer les facteurs qui influent sur la résistance au cisaillement qu'offrent les joints par contact entre les poutres de béton prémoulées et les dalles de béton coulées en place. On s'est tracé un programme expérimental comportant une série d'essais sur 42 poutres et un certain nombre de cylindres: on a ensuite cherché à établir l'influence de chacun des facteurs suivants: degré de rugosité de la surface de contact, longueur sur laquelle les contraintes de cisaillement se développent, pourcentage d'armature disposée en travers du joint, présence de clavettes (ou clés de cisaillement), position du joint par rapport à l'axe neutre de la poutre et résistance du béton à la compression. Les résultats des essais indiquent qu'il existe des relations complexes entre le degré de rugosité de la surface de contact, la longueur sur laquelle les contraintes de cisaillement se développent et le pourcentage d'armature disposée en travers du joint.

Horizontale Schubverbindungen zwischen vorgefertigten Trägern und an Ort betonierten Platten

Dieses Projekt beschäftigte sich mit der Festigkeit von Verbindungen zwischen vorgefertigten Beton-Trägern und an Ort betonierten Platten. In dem Versuchsprogramm wurden 42 Träger und notwendige Kontroll-Zylinder geprüft, mit dem Zweck Informationen über folgende Variablen zu erhalten:

Grad der Kontakt-Oberflächen-Rauheit, Länge der Scherspannweite, Prozentsatz des Stahls durch die Verbindung, Einfluss von Verdübelungen, Position der Verbindung in Bezug auf die neutrale Axe, und die Druckfestigkeit des Betons. Die erhaltenen Resultate weisen komplexe Beziehungen zwischen der Rauheit der Oberflächenverbindung, Prozentsatz des Stahls durch die Verbindung und der Scherspannweite auf.

